

Calculating Modal Assurance Criteria from Electronic Holography Data

Karl A. Stetson, Karl Stetson Associates, LLC, Coventry Connecticut

This article illustrates the use of electronic holography to obtain data for calculating modal assurance criteria on blade-like structures. The test object was a flat aluminum plate clamped at one end. It was excited into each of its first 5 modes, and J_0 fringe data were converted to numerical data via a pseudo phase-step method. The plate was perturbed by fastening weights to either of the two free corners to simulate four modified blades. Modal assurance criteria were calculated for the unperturbed blade and the four perturbed conditions.

It is desirable that replacement blades for jet engines exhibit the same vibratory properties as the parts they are replacing to avoid vibratory fatigue failure during engine operation. While matching resonant frequencies has been important for many years, matching mode shapes is also becoming a concern. The ability to do this is facilitated by vibration measuring equipment such as laser vibrometers and electronic holography.

While both technologies offer accurate noncontact vibration measurement, they have significantly different features. Laser vibrometry scans the object under study with a laser beam and samples the reflected light. This light is combined with a frequency-shifted reference beam to generate a heterodyne signal, which is used to determine the vibration amplitude of the point on the object being illuminated. Modal frequency response may be detected by pointing the beam at a single point and scanning the sinusoidal excitation frequency of the object. Mode shapes may then be obtained by scanning the object surface at the frequency of each response peak obtained during the frequency scan.

By contrast, electronic holography is a full-field detection process where the entire object is illuminated with laser light and imaged onto a television camera. A reference beam is combined with the image beam, and the phase of the reference beam is stepped after each frame, usually by one-fourth of a phase cycle. The frames are captured in real time and processed to obtain the equivalent of a reconstructed hologram image of the object. When the object vibrates, the brightness of the image is modified by the square of a zero-order Bessel function of the first kind, J_0 . The argument of the Bessel function is proportional to the vibration amplitude of the object and where it is zero. At vibration nodes, the vibrating object appears as bright as the nonvibrating object. Within the antinodes, the zeros of the Bessel function generate fringes that connect points of common vibration amplitude. The fringes

may be converted to numerical data by introducing a matching phase modulation into the reference beam to shift the Bessel function fringes. A set of four shifted Bessel function fringe patterns can be used to create numerical data in a manner analogous to phase-step interferometry.¹ This process is described in detail in the next section.

With laser vibrometry, if the illuminated point on the object happens to lie at the node of one of the vibration modes, that mode may be missed during the frequency scan. Therefore, several frequency scans with different probe points may be required to assure that all modes are detected. With electronic holography, the entire object is seen at once, and the response of a vibration mode is usually very clear. Because electronic holography captures data simultaneously over the entire object, the number of available data points can exceed what is practical with laser vibrometry. Also, electronic holography has an advantage when the vibration modes have overlapping frequency response. In such cases, the actual response is the phasor sum of modes whose relative phase will vary with frequency. Near the peak resonance of one mode, the response of a combining mode will be very nearly 90° out of phase, and the response will consist of a standing wave component and a traveling wave component. Above or below the resonance of one mode, the other will combine either nearly in phase or out of phase with it and will modify its apparent mode shape. With the entire object in view, it is much easier to identify and eliminate these phenomena and obtain true vibration mode data for numerical evaluation.

Quantitative Holographic Analysis

Our company manufactures an electronic holography system (K/100 system with the HoloFringe300K computer program) that was used for this experiment. A description of the steps provided by its operating program will help one understand the process for vibration data recording. The computer controls a dual-channel, phase-adjustable frequency generator, and one channel supplies sinusoidal excitation to the test object, while the other provides sinusoidal excitation at the same frequency to a piezo-electric mirror in the reference beam.

Step 1. The program first records an image of the object without vibration to serve as a mask during phase unwrapping. It is assumed that image points below a certain threshold will lie outside the object and points above it will lie within the object. But the mask can be edited to eliminate points that are ambiguous or troublesome, or to draw a mask covering the object.

Step 2. The program then displays a stan-

dard time-averaged hologram in real-time, which the user can observe to locate the vibration mode and identify its frequency of maximum response. The user is instructed to adjust the amplitude until no more than the fifth zero of the J_0 function is displayed, because beyond that level, the amplitude of J_0^2 function may be too low to provide accurate data.

Step 3. The program switches control to the bias vibration generator, and the user is instructed to increase its *amplitude* until the zero-order fringe disappears and then to adjust its *phase* until it returns with maximum brightness. The range over which the zero-order fringe can be seen is actually quite broad, and it is typical to find phase values below and above this point where the zero-order fringe appears equal in brightness to its neighbors and then take the average of those values. The program is set up to instruct the user to find those two values in sequence and then sets the phase to the average of the two.

Step 4. The excitation to the object is turned off, and the user is instructed to increase the bias amplitude until the image appears as black as possible. This corresponds to the first zero of the J_0 function at an argument value of 2.4048. The program captures that value upon transition to the next step. The bias amplitudes used in the final data capture are calculated from this captured value.

Step 5. The program then proceeds to capture an image of the vibrating object without bias vibration and asks the user to mark a point on the zero-order fringe. This point is used to tell the unwrapping program where the unwrapped phase function should be approximately zero.

Step 6. After this point is marked, the program then captures four interferograms at bias levels corresponding to an equivalent phase shift of 135°, 45°, -45°, and -135° relative to the periodicity of the J_0^2 function. The interferograms are processed by a standard four-step algorithm, and the wrapped phase function is displayed. In addition, a set of images is created from these data for use in phase unwrapping.

Step 7. The program instructs the user to save this dataset for unwrapping by a program based on calculated unwrap regions.² The phase unwrap program first adds multiples of 2π to the values of the wrapped phase function to obtain a smooth phase function. The entire unwrapped phase function is then shifted by a multiple of 2π so that the values around the point that was marked as lying on the zero-order fringe are as close to zero as possible. The unwrapped phase function is then read through a look-up table that corrects for the fact that the J_0 function is not actually a cosine function. The final data are stored in two files, a *.out file that contains 16-bit pixels, where values of 256 corresponds to one cycle of a phase, and a *.img file that has 8-bit pixels scaled so that the minimum value is 0 and the maximum value is 255. This latter file is used to display the resulting phase function.

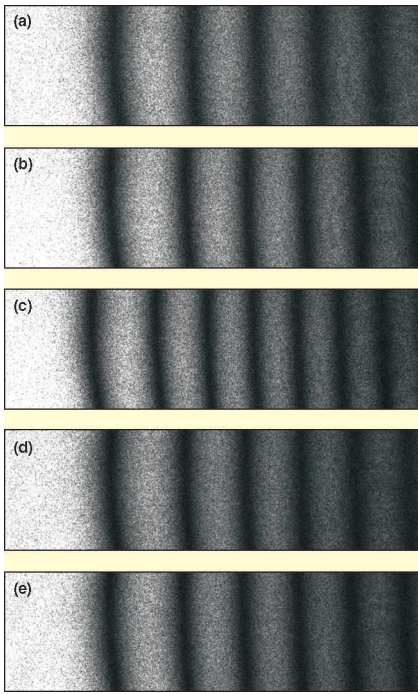


Figure 1. (a) Blade 1, Mode 1, 139.4 Hz (b) Blade 2, Mode 1, 136.8 Hz (c) Blade 3, Mode 1, 136.9 Hz (d) Blade 4, Mode 1, 134 Hz (e) Blade 5, Mode 1, 134.3 Hz.

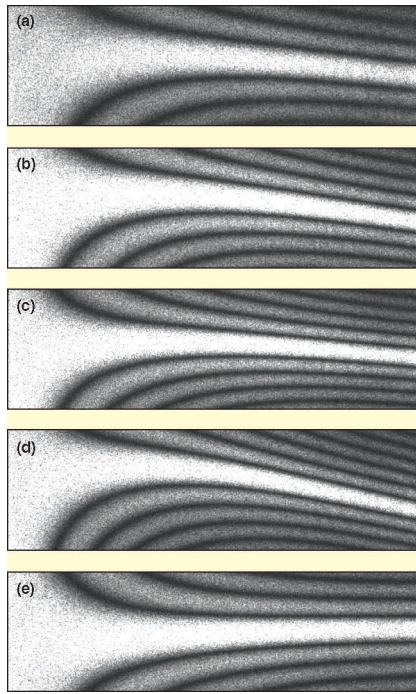


Figure 3. (a) Blade 1, Mode 3, 998 Hz (b) Blade 2, Mode 3, 983 Hz (c) Blade 3, Mode 3, 980 Hz (d) Blade 4, Mode 3, 956 Hz (e) Blade 5, Mode 3, 974 Hz.

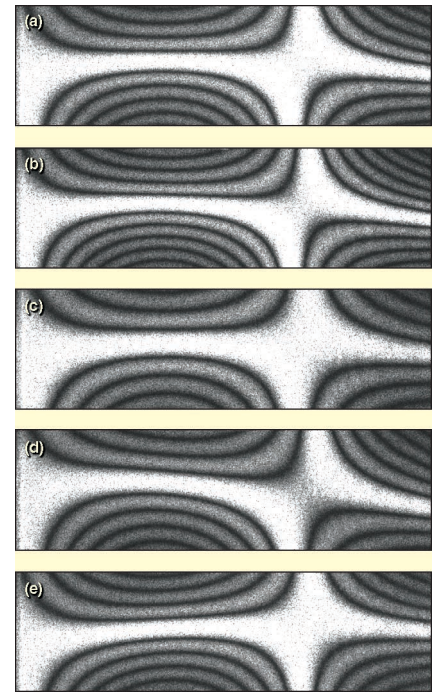


Figure 5. (a) Blade 1, Mode 5, 3112 Hz (b) Blade 2, Mode 5, 3053 Hz (c) Blade 3, Mode 5, 3041 Hz (d) Blade 4, Mode 5, 2954 Hz (e) Blade 5, Mode 5, 2995 Hz.

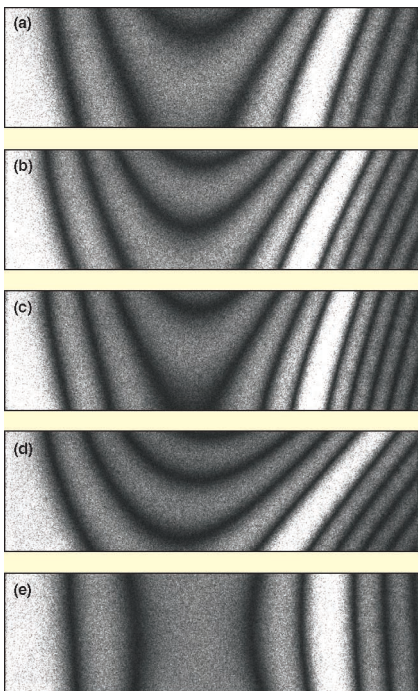


Figure 2. (a) Blade 1, Mode 2, 888 Hz (b) Blade 2, Mode 2, 874 Hz (c) Blade 3, Mode 2, 874 Hz (d) Blade 4, Mode 2, 866 Hz (e) Blade 5, Mode 2, 853 Hz.

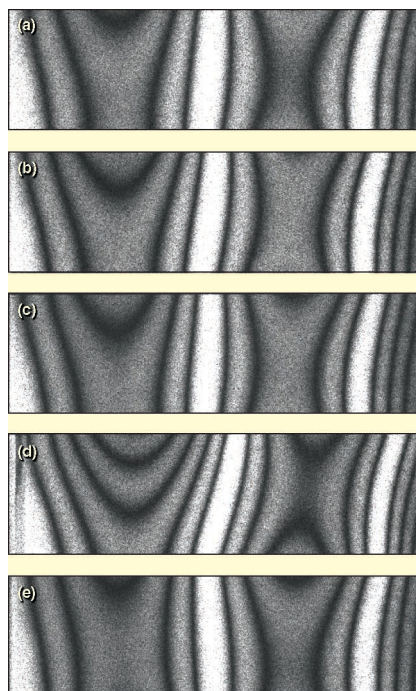


Figure 4. (a) Blade 1, Mode 4, 2468 Hz (b) Blade 2, Mode 2, 874 Hz (c) Blade 3, Mode 2, 874 Hz (d) Blade 4, Mode 2, 866 Hz (e) Blade 5, Mode 2, 853 Hz.

MAC and Holographic Analysis

The primary purpose of this article is to illustrate the use of electronic holography data in calculations of modal assurance criteria (MAC), which are commonly used to quantify the similarity of vibration mode patterns on similar but different objects.³ We will designate two similar vibration patterns for two separate structures as Ψ_1 and Ψ_2 . In general these will be vectorial quantities, but for holography or laser vibrometry systems with a single perspective,

they will be scalars. The MAC calculation for these two patterns is:

$$\text{MAC} = \frac{[\sum \Psi_1 \Psi_2]^2}{[\sum \Psi_1^2 \sum \Psi_2^2]} \quad (1)$$

where Σ indicates a summation over the number of data points on the object. Note that this calculation is self-normalizing, and any factor multiplying either pattern will be canceled, allowing the MAC values to range from 0 to 1.

To apply this calculation to holographic vibration analysis data, several things must

be considered. First, the images of both objects should be the same size in the data file. This can be accomplished by locating both objects the same distance from the holographic optical head to eliminate variation of image size. The holography system used in this work uses a zoom lens to provide images of the objects under study, and it is essential that the zoom lens magnification remain constant throughout such tests. It is also necessary that the two objects exhibit no relative rotation. Small shifts in vertical or horizontal position are accounted for by software analysis. The same image file that is used for guiding the phase unwrap program is used to define the valid location of the object for the MAC calculations.

Experimental Data

A flat aluminum plate 153 mm long by 38 mm wide by 3 mm thick was chosen to approximate the shape of a blade. It was clamped at one end for a length of 24 mm to simulate the mounting of a bladed disk. The clamping vise was cemented to a translation stage so that misregistration could be simulated. The plate was modified by fixing a weight to either of the free corners. The use of two weights, 0.15 g and 0.7 g, placed in either of the two positions allowed simulation of four departures from the modal structure of the unperturbed plate. The weight of the entire plate, including the clamped section, was 47.7 g.

Figures 1 through 5 show the five vibration modes recorded as J_0 fringes for the five conditions of the plate, which have been designated as different blades, Blades 1, 2, 3, 4, and 5. The images have been organized to show Mode 1 for Blades 1 through 5 in one column, Mode 2 for Blades 1 through 5 in the next column, etc. This allows com-

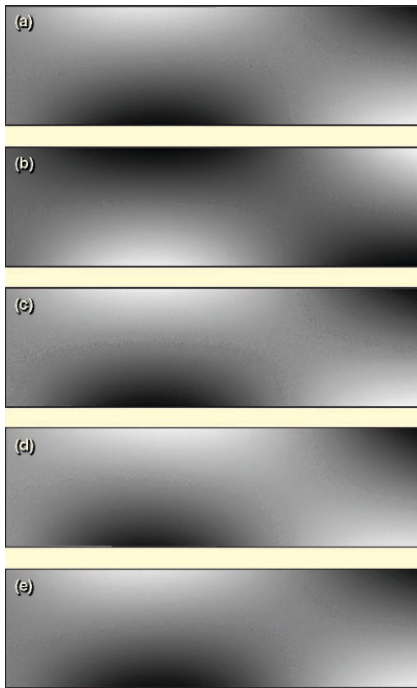


Figure 6. Image data: (a) Blade 1, Mode 5 (b) Blade 2, Mode 5 (c) Blade 3, Mode 5 (d) Blade 4, Mode 5 (e) Blade 5, Mode 5.

parison of how the modes have changed with the perturbation. Figures 6a through 6e show *.img file images of the data for the fifth modes of Blades 1 through 5, and they are located to the right of their corresponding J_0 images.

Discussion

Table 1 shows an array of the calculated MAC values for the five blades and their corresponding five modes. The values of 1.0 in the first column are the result of MAC calculations comparing Blade 1 to itself via exactly the same data files. The values of 0.998 for the first row in the row labeled Mode 1 show that very little change occurred to that mode shape due to any of the four mass perturbations. The values in Columns 2 and 3 are also quite high and indicate that the perturbations due to the 0.15-gram weight had very little effect, if any, on the mode shapes. However, the values in Columns 4 and 5 show some significant effect, and this is expected from looking at the mode shapes shown in Figures 1-5.

Table 1. MAC calculations for five modes of five blades shown in Figures 1 through 5.

	Blade 1	Blade 2	Blade 3	Blade 4	Blade 5
Mode 1	1.0	0.998	0.998	0.998	0.998
Mode 2	1.0	0.992	0.995	0.957	0.953
Mode 3	1.0	0.982	0.984	0.949	0.925
Mode 4	1.0	0.994	0.994	0.981	0.986
Mode 5	1.0	0.993	0.988	0.967	0.969

Table 3. Admixture coefficients for mass perturbation of modes of test plate.

	Frequency	Blade 1	Blade 2	Blade 3	Blade 4	Blade 5
Mode 1	139	1.000	0.025	0.020	0.003	0.002
Mode 2	888	0.025	1.000	3.801	0.149	0.089
Mode 3	998	0.020	3.801	1.000	0.196	0.115
Mode 4	2463	0.003	0.149	0.196	1.000	1.677
Mode 5	3112	0.002	0.089	0.115	1.677	1.000

In assessing the numbers in Table 1, it is desirable to have an indication of what constitutes the maximum MAC value that can be expected between two blades that are identical in all respects except for the microstructure of their surfaces. When illuminated with laser light, the unique microstructure of a surface will give rise to a unique microstructure in the reflected light, which is referred to as a speckle pattern. This in turn gives rise to a noisy fluctuation in the values of vibratory displacement in the data captured by this system.

To get an estimate of the level of error that this effect can create, the same five vibration modes were recorded of the unperturbed blade in two lateral positions relative to the holography system. The translation, in the order of 2.5 mm, was enough to completely decorrelate the reflected speckle pattern, which depends on illumination angle, and yet, since the plate itself was unchanged, simulate two distinct but identical structures. Table 2 shows the results of MAC calculations for these five modes. The effect of this source of error is less than one percent.

Prediction of Mode Shape Changes

Changes in mode shapes and frequencies can be estimated by perturbation theory.⁴ For a purely mass perturbation, as in this case, the frequency change can be expressed as:

$$\Delta f_n / f_n = \Delta M_n / M_n \quad (2)$$

where:

M_n = modal mass of n th mode number, defined as the integral of mass density times Ψ_n^2

ΔM_n = integral of the perturbing mass distribution times Ψ_n^2

f_n = frequency of the mode

Δf_n = change in modal frequency

The change in any mode shape can be expressed as an admixture of the original mode shape and small amounts of all the other original modes according to the matrix equation:

$$[\Psi'_n] = [C_{nk}][\Psi_n] \quad (3)$$

where the prime denotes the perturbed modes, and C_{nk} are the admixture coef-

Table 2. Flat plate compared with itself shifted by 2.5 mm.

	Blade 1	Blade 2
Mode 1	1.0	0.998
Mode 2	1.0	0.997
Mode 3	1.0	0.994
Mode 4	1.0	0.993
Mode 5	1.0	0.992

ficients. The diagonal elements of the C matrix are unity, and the off-diagonal elements are defined as:

$$C_{nk} = (\Delta M_{nk} / M_k) / (f_k^2 / f_n^2 - 1) \quad (4)$$

and

$$C_{kn} = (\Delta M_{nk} / M_n) / (f_n^2 / f_k^2 - 1) \quad (5)$$

where ΔM_{nk} is the integral of the distribution of perturbing mass times the product $\Psi_n \Psi_k$. C_{kn} and C_{nk} are both the amount of mode k subsumed by mode n due to the perturbation; however, C_{nk} is used for modes higher in frequency than the mode considered, while C_{kn} is used for those lower in frequency.

For a given mass perturbation, the frequency factor in Eqs. 4 and 5 gives an indication of how modes are most likely to be affected by a given mass perturbation. Clearly, the closer two modes are in frequency, the more likely they will admix due to the perturbation. Calculation of the admixture coefficients for these five modes leads to Table 3).

Mode 1 has very small admixture coefficients; therefore, we do not expect much change in its mode shape. The admixture coefficients between modes 2 and 3 are the highest, followed by those between Modes 4 and 5. These predictions are in reasonable agreement with the MAC data in Table 1.

Conclusion

Electronic holography provides an efficient method for identifying vibration modes of structures and recording vibration modes as numerical data in a form usable for modal assurance criteria calculations. As such, it is a viable alternative to laser vibrometry for this application.

References

1. Stetson, K. A., Brohinsky, W. R., "A Fringe Shifting Technique for Numerical Analysis of Time-Average Holograms of Vibrating Objects," *J. Opt. Soc. Amer. A*, Vol. 5, pp. 1472-1476, 1988.
2. Stetson K. A., Wahid J., Gauthier P., "Noise-Immune Phase Unwrapping by Use of Calculated Wrap Regions," *Appl. Opt.*, Vol. 36, pp. 4830-4838, 1997.
3. Allemang R. J., "The Modal Assurance Criterion - 20 Years of Use and Abuse," *J. of Sound and Vibration*, Vol. 37, No. 8, pp. 14-21, 2003.
4. Stetson K. A., "Perturbation Method of Structural Design Relevant to Holographic Vibration Analysis," *AIAA Journal*, Vol. 13, pp. 457-459, 1975.

Please visit www.pcholo.com for more information on the K/100 system with HoloFringe300K computer program

The author can be reached at: kastetson@snet.net.